

Poly(ADP-ribose) Polymerase-1 Hyperactivity at DNA Single-Strand Breaks Triggers Seizures and Shortened Lifespan

Emilia Komulainen¹, Stephanie Rey², Stuart Rulten¹, Limei Ju¹, Peter J. McKinnon³, Kevin Staras², and Keith W Caldecott¹

¹Genome Damage and Stability Centre, School of Life Sciences, University of Sussex, Falmer, Brighton, BN1 9RQ

²Sussex Neuroscience, School of Life Sciences, University of Sussex, Falmer, Brighton, BN1 9QG

³Dept. Genetics, St Jude Children's Research Hospital, Memphis, Tennessee, USA 38105

To whom correspondence should be addressed; k.w.caldecott@sussex.ac.uk or k.staras@sussex.ac.uk

Defects in DNA strand break repair can trigger seizures that are often intractable and life-threatening. However, the molecular mechanism/s by which unrepaired DNA breaks trigger seizures are unknown. Here, we show that hyperactivity of the DNA break sensor protein poly(ADP-ribose) polymerase-1 is widespread in DNA single-strand break repair defective *XRCC1*-mutant mouse brain, including the hippocampus and cortex. We demonstrate elevated seizure-like activity in *XRCC1*-mutant hippocampus in vitro and increased seizures in vivo, and we show that *Parp1* deletion reduces or prevents both. We also show that the increased seizures in *Xrcc1* mutant mice result in juvenile mortality, and that *Parp1* deletion extends the lifespan of these mice up to 25-fold. *Parp1* hyperactivation is thus a major molecular mechanism by which unrepaired endogenous DNA strand breaks trigger disease pathology, including neurological seizures and death. These data implicate inhibitors of PARP activity as a possible therapeutic approach for the treatment of single-strand break induced neurodegenerative disease.

DNA single-strand breaks (SSBs) are the commonest lesions arising in cells and can result directly from damage to deoxyribose, indirectly as an obligate intermediate of DNA base or ribonucleotide excision repair, and as abortive intermediates of topoisomerase activity. SSBs are rapidly detected by the enzymes poly(ADP-ribose) polymerase-1 (PARP1) and/or poly(ADP-ribose) polymerase-2 (PARP2); two enzymes that bind to DNA breaks and subsequently modify themselves and other proteins at the site of the break with polymeric chains of ADP-ribose (1-3). This polymer, denoted poly(ADP-ribose), triggers recruitment the DNA single-strand break repair (SSBR) scaffold protein XRCC1 and its protein partners which subsequently can process any damaged DNA termini at the break and complete SSBR (4-6).

If not repaired rapidly, SSBs can result in replication fork stalling and/or collapse (7-10) and can block the progression of RNA polymerases during gene transcription (11, 12). Moreover, mutations in proteins involved in SSBR are associated in humans with cerebella ataxia, neurodevelopmental defects, and episodic seizures (13-19). To date, all of the identified SSBR-defective human diseases are mutated in either

XRCC1 or in one of its protein partners (17). Seizures in humans are often intractable, progressive, and can result in premature death, a phenomenon known as Sudden Death During Epilepsy (SUDEP). However, nothing is known about the molecular mechanism/s by which unrepaired DNA strand breaks trigger these events.

Recently, we demonstrated using the *Xrcc1^{Nes-Cre}* mouse model that SSBR-defective cerebellum possesses elevated steady-state levels of poly(ADP-ribose) resulting from the hyperactivation of PARP1 and leading to the loss of cerebellar interneurons and ataxia(17, 20). PARP1 hyperactivity has been proposed trigger cytotoxicity by several mechanisms including excessive depletion of NAD⁺/ATP, inhibition of glycolysis, and/or by a specialised type of apoptosis triggered by excessive levels of poly(ADP-ribose) known as parthanatos (21-26). However, the extent to which PARP1 hyperactivation impacts on neurological function in response to endogenous DNA damage is unknown. Here, we have addressed this question. Strikingly, we show that elevated levels of poly(ADP-ribose) extend beyond the cerebellum and are widespread across SSBR-defective brain, including the cortex and hippocampus. We show that *Parp1* deletion ablates poly(ADP-ribose) accumulation in SSBR-defective brain and elevated seizures both in vitro and in vivo. We also show that *Parp1* deletion prevents juvenile mortality in *Xrcc1^{Nes-cre}* mice, extending their life-span up to 25-fold. These data identify PARP1 hyperactivation as a major molecular mechanism by which endogenous DNA damage triggers neurological seizures and death.

Results

Poly(ADP-ribose) levels are elevated throughout single-strand break repair-defective brain. To examine the extent to which PARP1 hyperactivity might underlie the neuropathology induced by endogenous single-strand breaks (SSBs) we measured the steady-state level of ADP-ribose across *Xrcc1^{Nes-cre}* mouse brain by immunohistochemistry. Strikingly, we detected increased levels of ADP-ribose throughout *Xrcc1^{Nes-cre}* brain, including the cerebral cortex, with anti-ADP-ribose immunostaining particularly strong in the cerebellum and hippocampus (Fig.1a & 1b). The elevated anti-ADP-ribose signal resulted from PARP1 activity because *Parp1* deletion in *Xrcc1^{Nes-cre}* mice reduced this signal to levels similar to or below those in

wild-type brain (Fig.1b; *Parp1*^{-/-}/*Xrcc1*^{Nes-cre}). Notably, we did not observe elevated ADP-ribose immunostaining in brain from *Ku70*^{-/-} mice, in which non-homologous end-joining (NHEJ) is defective (Fig.1a & 1b). NHEJ is the primary if not only pathway available for repair of DNA double-strand breaks in postmitotic cells (27, 28), confirming that the elevated poly(ADP-ribose) *Xrcc1*^{Nes-cre} brain is a reflection of unrepaired SSBs and not DSBs.

That we detected endogenous poly(ADP-ribose) across *Xrcc1*^{Nes-Cre} brain was surprising, because in cultured cell lines the level of this polymer is normally detected only following exogenous DNA damage, even in XRCC1-defective cells (17). This suggests that endogenous SSBs arise more frequently in brain than in cultured cells, perhaps in part explaining why diseases in which SSBR is defective are associated primarily with neurodegeneration. The presence of elevated poly(ADP-ribose) in *Xrcc1*^{Nes-Cre} hippocampus was of particular interest, because defects in this region of the brain are often associated with increased seizure activity (29). The elevated poly(ADP-ribose) in *Xrcc1*^{Nes-cre} hippocampus was primarily if not entirely present in neuronal nuclei, consistent with the nuclear defect in SSBR (Fig.2a, top panels), and was present as discrete nuclear foci, presumably reflecting sites at which unrepaired endogenous SSBs are induced and/or concentrated. We also detected elevated levels of γ H2AX in *Xrcc1*^{Nes-cre} hippocampus, albeit at much lower levels than poly(ADP-ribose), consistent with previous results (20) and further indicative of the presence of unrepaired DNA damage (Fig.2a). Interestingly, whereas the elevated poly(ADP-ribose) was ablated by deletion of *Parp1*, the presence of γ H2AX was not. This confirms that whilst deletion of the SSB sensor protein ablates poly(ADP-ribose) signalling at unrepaired SSBs in *Xrcc1*^{Nes-cre} mice it does not rescue the DNA repair defect.

PARP1 hyperactivation at unrepaired single-strand breaks triggers seizures in vitro and in vivo. To examine directly whether loss of *Xrcc1*-dependent SSBR results in elevated seizure activity in hippocampus we conducted electrophysiological experiments. Continuous extracellular recordings were made from the hippocampal CA3 region of acute brain slices during perfusion into an epileptogenic solution, and the onset of seizure-like events was recorded. Seizure-like activity was indeed significantly higher in *Xrcc1*^{Nes-Cre} hippocampus in these experiments, with this activity

beginning sooner and occurring more frequently over the time course of the experiment (Fig.2b). Indeed, the mean cumulative number of seizure-like events was ~4-fold greater in hippocampus from *Xrcc1^{Nes-Cre}* mice than in wild type mice (Fig.2c & 2d). Importantly, this elevated seizure activity was reduced and/or prevented if one or both alleles of *Parp1* were deleted, implicating Parp1 hyperactivity as a cause of the elevated seizure activity in SSBR-defective hippocampus, *in vitro* (Fig.2c & 2d).

Next, we examined whether Parp1 activity is similarly responsible for the elevated seizures reported in *Xrcc1^{Nes-Cre}* mice, *in vivo*. Since the seizures in *Xrcc1^{Nes-Cre}* mice are sporadic, we monitored *Xrcc1^{Nes-Cre}* mice by infrared video imaging and recorded the frequency of seizures for a four-day period, from P15. In contrast to wild type mice, in which we failed to observe any seizures, *Xrcc1^{Nes-Cre}* mice exhibited numerous mild/moderate seizures during the same timespan (Fig.3a). Moreover, the seizures became more frequent and/or severe during the course of the experiment, ultimately resulting in a terminal seizure and death (Fig.3a). Seizures have similarly been associated with death in humans, resulting in a condition denoted Sudden Unexpected Death During Epilepsy (SUDEP)(30, 31). Importantly, we failed to detect seizures over the same time period in *Xrcc1^{Nes-Cre}* mice in which one or both *Parp1* alleles were deleted (Fig.3a). These data indicate that Parp1 hyperactivation triggers seizure activity in the absence of efficient SSBR not only *in vitro*, but also *in vivo*. To our knowledge, this is the first demonstration that seizure activity can be triggered by Parp1 activity.

PARP1 deletion prevents juvenile mortality in single-strand break repair-defective mice. The cause of death in *Xrcc1^{Nes-Cre}* mice during seizure is unclear but, similar to SUDEP, is likely to result from the disruption of normal cardiac or respiratory function (32). Moreover, the observation of fatal seizures in *Xrcc1^{Nes-Cre}* mice provides a plausible explanation for the juvenile mortality reported previously in this mouse model (33). To test this directly, we examined the impact of *Parp1* deletion on the lifespan of *Xrcc1^{Nes-Cre}* mice. The median lifespan of *Xrcc1^{Nes-Cre}* mice in our cohort was ~3-4 weeks, consistent with the age at which we detected terminal seizures by video imaging (Fig.3b). Moreover, the longevity of *Parp1^{+/-}/Xrcc1^{Nes-Cre}* and *Parp1^{-/-}/Xrcc1^{Nes-Cre}* littermates in which one or both *Parp1* alleles were additionally deleted was increased ~7-25 fold; with median lifespans of 23 and 79 weeks, respectively (Fig.3b). That deletion of one *Parp1* allele prolonged the lifespan of *Xrcc1^{Nes-Cre}* mice to a

greater extent than deletion of both *Parp1* alleles suggests that whereas loss of one *Parp1* allele is sufficient to suppress Parp1-induced cytotoxicity, loss of the second allele eradicates an additional role for Parp1 in *Xrcc1*-defective brain that is important for survival.

Discussion

DNA single-strand breaks (SSBs) arise in cells several orders of magnitude more frequently than DNA double-strand breaks (DSBs) and if not repaired rapidly these lesions can block the progression of DNA and RNA polymerases (17). The collision of DNA polymerases with SSBs during DNA replication can result in replication fork collapse and the formation of DSBs (8-10, 34, 35). However, cells possess effective and accurate homologous recombination mechanisms by which replication-associated DSBs can be repaired using an intact sister chromatid (36-38), perhaps explaining why human diseases in which SSBR is attenuated do not result in markedly elevated genome instability and cancer. Consistent with this idea, cells from individuals with genetic defects in SSBR possess elevated levels of sister chromatid exchange; a hallmark of homologous sister chromatid recombination (16, 17). In contrast, post-mitotic cells lack sister chromatid recombination and so are more reliant on SSBR, most likely explaining why defects in the latter pathway are primarily associated with neurological dysfunction.

Arguably the most severe pathology arising in SSBR-defective disease are neurological seizures. However, the molecular mechanisms by which unrepaired DNA single-strand breaks trigger these events are unknown. Here, we have identified one such mechanism. We reveal that levels of poly(ADP-ribose) are elevated across *Xrcc1^{Nes-Cre}* brain, with high levels particularly evident in cerebellum and hippocampus; regions of the brain associated with seizure activity. The presence of elevated poly(ADP-ribose) is consistent with the SSBR defect in *Xrcc1^{Nes-Cre}* mice, because the synthesis of this polymer by poly(ADP-ribose) polymerases is triggered by SSBs (2, 3, 39). Nevertheless, that endogenous poly(ADP-ribose) is detectable in *Xrcc1^{Nes-Cre}* brain is surprising because in cultured cell lines the level of this polymer is normally detected only following exogenous DNA damage, even in XRCC1-defective cells. One possible explanation is that some sources of stochastic SSBs arise at much higher

frequencies in brain than in cultured cells. For example, one possible source of SSBs arising specifically in brain are those resulting from elevated oxidative stress during glutamate excitotoxicity (40, 41).

In addition to stochastic sources, it is also possible that SSBs arise in a 'programmed' manner in brain as a result of elevated topoisomerase activity and/or base excision repair associated with gene transcription and/or epigenetic reprogramming. For example, the abortive activity of topoisomerase I during gene transcription results in protein-linked SSBs that require SSBR for removal, and defects in the repair of these lesions is implicated in neurodegenerative disease (16, 19). Similarly, epigenetic reprogramming involves removal of 5'-methylcytosine and 5'-hydroxymethylcytosine by mechanisms that employ base excision repair, during which SSBs are an obligate intermediate. Whilst such breaks have not yet been implicated in neurodegenerative disease, 5-hydroxymethylcytosine is highly enriched in brain (42, 43).

These data are the first to demonstrate a molecular mechanism by which unrepaired DNA strand breaks trigger neurological seizures. Seizures are potentially lethal events, associated with a condition denoted Sudden Unexpected Death During Epilepsy (SUDEP) (30, 31). Indeed, *Xrcc1^{Nes-Cre}* mice exhibit a dramatically shortened lifespan, which we have now established by video imaging is due to episodic epilepsy leading ultimately to a fatal seizure. The cause of death in *Xrcc1^{Nes-Cre}* mice during seizure is unclear but, similar to SUDEP, is likely to result from the disruption of normal cardiac or respiratory function (32). The discovery that genetic deletion of one or both *Parp1* alleles increased lifespan of *Xrcc1^{Nes-Cre}* mice by 7-25 fold is striking. Surprisingly, deletion of one *Parp1* allele prolonged the lifespan of *Xrcc1^{Nes-Cre}* mice to a greater extent than did deletion of both *Parp1* alleles. This indicates that whereas loss of one allele of *Parp1* is sufficient to suppress Parp1-induced cytotoxicity, additional loss of the second allele eradicates an as yet unidentified role for Parp1 in *Xrcc1*-defective brain that is important for long-term survival.

To our knowledge, the level of life-span extension observed in these experiments is unprecedented in a DNA repair-defective mouse, and is particularly notable in that the level of DNA damage in *Xrcc1^{Nes-Cre}* brain is not reduced by *Parp1* deletion. There are a number of reported mechanisms by which PARP1 hyperactivity can trigger cell death including excessive depletion of NAD⁺, inhibition of glycolysis, and/or by a specialised type of apoptosis known as Parthanatos (21-26). It will now be

of interest to determine which of these mechanisms is triggered in XRCC1-defective brain.

In summary, we reveal here that Parp1 hyperactivity is a major molecular mechanism by which seizures and shortened lifespan are triggered by endogenous unrepaired DNA single-strand breaks.

Figure Legends

Fig.1. Global hyperactivation of PARP1 in SSBR-defective *Xrcc1*^{-/-} brain. (a), Sagittal sections obtained from mice of the indicated genotypes were immunostained for ADP-ribose. The regions of most prominent staining in XRCC1-defective brain (cerebellum and hippocampus) are boxed. (b), Magnified images of sagittal sections showing levels of ADP-ribose in the hippocampal regions CA1, CA2, and dentate gyrus (DG), and in the cortical layers L2/3 and L5. Scale bars 5mm (A), 50µm (B).

Fig.2. PARP1 hyperactivation triggers seizure-like activity *in vitro* in *Xrcc1*^{Nes-Cre} brain. (a), *Left*, immunofluorescence images of ADP-ribose and γ H2AX (a measure of DNA damage) in the hippocampal CA3 region of mouse brain of the indicated genotypes. *Right*, quantitation of γ H2AX levels in the above experiments; *Xrcc1*^{+/+} (n = 85 cells, 3 mice), *Xrcc1*^{Nes-Cre} (n = 114 cells, 3 mice), *Parp1*^{+/-} *Xrcc1*^{Nes-Cre} (n = 100 cells, 2 mice), *Parp1*^{-/-} *Xrcc1*^{Nes-Cre} (n = 85 cells, 4 mice) and *Parp1*^{-/-} *Xrcc1*^{+/+} (n = 51 cells, 2 mice). Statistically significant differences were determined using paired two-tailed t-tests (**p<0.0001). (b), Example voltage traces showing seizure-like events (SLEs) in the hippocampal CA3 region of acute brain slices from *Xrcc1*^{+/+} and *Xrcc1*^{Nes-Cre} mice following incubation in an epileptogenic solution. A cartoon of the experimental approach is shown, *top left*. (c), Heatplot timelines showing cumulative SLE's for each experiment in brain slices of the indicated genotypes. Each horizontal bar corresponds to one brain slice with color-coding indicating cumulative SLEs (0-190) in two-minute bins. (d), Plot of the mean (\pm s.e.m) cumulative SLE's in brain slices of the indicated genotypes from all experiments; *Xrcc1*^{Nes-Cre} (n = 12 slices), *Parp1*^{+/-} *Xrcc1*^{Nes-Cre} (n = 12), *Xrcc1*^{+/+} (n = 11), *Parp1*^{-/-} *Xrcc1*^{Nes-Cre} (n = 10). At recording endpoint, the mean cumulative SLE's in *Xrcc1*^{Nes-Cre} hippocampus is significantly higher than in *Xrcc1*^{+/+}

and $Parp1^{-/-}/Xrcc1^{Nes-Cre}$ hippocampus (one-way ANOVA, $P < 0.0001$, Tukey's pairwise comparisons, $P < 0.001$).

Fig.3. PARP1 hyperactivation triggers juvenile seizures and mortality in the absence of XRCC1. (a), Video monitoring and recording of generalised running/bouncing seizures in mice of the indicated genotypes from P15-P19. The point of death of $Xrcc1^{Nes-Cre}$ mice by fatal seizure is indicated (cross). Note that we did not detect any seizures in mice of other genotypes in the experiment. $Xrcc1^{+/+}$ (n = 9 mice), $Xrcc1^{Nes-Cre}$ (n = 3 mice), $Parp1^{+/-}/Xrcc1^{Nes-Cre}$ (n = 3 mice), and $Parp1^{-/-}/Xrcc1^{Nes-Cre}$ (n = 3 mice). (b), Kaplan-Meier curve for survival of mice of the indicated genotypes. The table shows number of individuals in each group, median survival in weeks, and p-values from pairwise curve comparisons (Log-rank Mantel-Cox tests).

Acknowledgements. This work was funded by an MRC Programme grant to KWC and KS (MR/P010121/1) and a BBSRC Project grant to KS (BB/K019015/1). We thank Zhao-Qi Wang for the $Parp1^{-/-}$ mouse strain.

Methods

Animals and animal care. Experiments were carried out in accordance with the UK-Animal (Scientific Procedures) Act 1986 and satisfied local institutional regulations at the University of Sussex. Mice were maintained and used under the auspices of UK Home Office project license number P3CDBCBA8. The generation of $Parp1^{-/-}$, $Xrcc1^{Nes-Cre}$, and $Ku70^{-/-}$ mice were reported previously (17, 20, 44). Intercrosses between $Parp1^{-/-}$ and $Xrcc1^{+/loxP}$ mice were maintained in a mixed background C57Bl/6 × S129 strain and housed on a 12 h light/dark cycle with lights on at 7:00. Temperature and humidity were maintained at 21 °C (± 2 °C) and 50% ($\pm 10\%$), respectively. All experiments were performed under the UK Animal (Experimental Procedures) Act, 1986.

Immunohistochemistry and microscopy. Antibodies used were rabbit Fc-fused Anti-pan-ADP-ribose binding reagent Millipore; MABE1016), anti- γ H2AX mouse monoclonal (Millipore; 05-636). Secondary antibodies used for immunofluorescence

were donkey anti-mouse Alexa 568 and anti-rabbit Alexa 488 (Invitrogen; A10037 and A21206), and for immunohistochemistry Biotin-SP-conjugated AffiniPure goat anti-rabbit antibody (JacksonImmuno Research; 111-065-144). Mice (P15) were anaesthetized using 0.25 mg/g Dolethal (Vetoquinol UK Ltd) and perfused transcardially with PBS followed by 4% formaldehyde. Brains were postfixed in 4% paraformaldehyde for 48 h and stored in 25% sucrose/PBS until moulding and freezing (TFM-5). 10-20 μm sagittal sections were prepared using a cryostat (Leica CM1850). Immunohistochemistry was conducted as described previously(17). Fluorescent images were acquired using the Zeiss LSM880 confocal microscope, with oil immersion objective (Plan-Apochromat 63 \times /1.4 Oil DIC M27). The Airyscan super-resolution module was used to obtain high-resolution images. The image stacks were deconvoluted using the Huygens Professional software version 4.4 (Scientific Volume Imaging, The Netherlands) and processed for brightness and contrast in ImageJ 1.51j. γH2AX foci were counted manually in z-stacks using ImageJ. Images of immunohistochemistry samples were acquired with the LSM880 using the wide-field imaging mode (Axiocam 503 Mono, Plan-Apochromat 10 \times /0.45 and 20 \times /0.8 M27). Whole tissue sections were imaged in a tiling mode with 10% overlap and stitched in Zeiss Zen blue.

Electrophysiology. Acute transverse hippocampal slices (300 μm) were prepared from P14-P16 mice using a vibroslicer (VT1200S, Leica Microsystems, Germany) in ice-cold artificial cerebrospinal fluid containing (in mM): 125 NaCl, 2.5 KCl, 25 glucose, 1.25 NaH_2PO_4 , 26 NaHCO_3 , 1 MgCl_2 , 2 CaCl_2 (bubbled with 95% O_2 and 5% CO_2 , pH 7.3). All experiments were performed at 23-25 $^\circ\text{C}$. During an experiment, an extracellular electrode was placed in the hippocampal CA3 pyramidal region and field voltage recordings made for 26 mins as slices were perfused from ACSF into a modified (epileptogenic) saline containing 125 NaCl, 5 KCl, 25 glucose, 1.25 NaH_2PO_4 , 26 NaHCO_3 , 2 CaCl_2 . Signals were amplified using a MultiClamp 700A (Molecular Devices), digitized at 50 kHz with a Digidata 1320 and recorded in pCLAMP acquisition software (Molecular Devices) for offline analysis.

Videoanalysis. Videomonitoring was performed using the Noldus PhenoTyper 3000 system, including infrared LED units and a video recording camera for the duration of the experiment (Video output CCIR black/white VPP -75 Ohm (PAL) or EIA black/white

Vpp-75 Ohm (NTSC)). Mice were placed in the chamber with floor area 30cm x 30cm and were provided with bedding, minimal nesting, food pellets and a water source. Mouse pups of the indicated genotype were housed with mother and a control sibling from P15 up to P20. Video recordings were observed after recording and the number of running-bouncing-seizures was quantified.

1. Amé JC, et al. (1999) PARP-2, A novel mammalian DNA damage-dependent poly(ADP-ribose) polymerase. *J Biol Chem* 274(25):17860–17868.
2. Benjamin RC, Gill DM (1980) ADP-ribosylation in mammalian cell ghosts. Dependence of poly(ADP-ribose) synthesis on strand breakage in DNA. *J Biol Chem* 255(21):10493–10501.
3. Ikejima M, et al. (1990) The zinc fingers of human poly(ADP-ribose) polymerase are differentially required for the recognition of DNA breaks and nicks and the consequent enzyme activation. Other structures recognize intact DNA. *J Biol Chem* 265(35):21907–21913.
4. El-Khamisy SF, Masutani M, Suzuki H, Caldecott KW (2003) A requirement for PARP-1 for the assembly or stability of XRCC1 nuclear foci at sites of oxidative DNA damage. *Nucleic Acids Res* 31(19):5526–5533.
5. Hanzlikova H, Gittens W, Krejcikova K, Zeng Z, Caldecott KW (2016) Overlapping roles for PARP1 and PARP2 in the recruitment of endogenous XRCC1 and PNKP into oxidized chromatin. *Nucleic Acids Res* 45(5):2546–2557.
6. Okano S, Lan L, Caldecott KW, Mori T, Yasui A (2003) Spatial and temporal cellular responses to single-strand breaks in human cells. *Mol Cell Biol* 23(11):3974–3981.
7. Single-strand interruptions in replicating chromosomes cause double-strand breaks. (2001) Single-strand interruptions in replicating chromosomes cause double-strand breaks. *98(15):8241–8246*.
8. Hsiang YH, Lihou MG, Liu LF (1989) Arrest of replication forks by drug-stabilized topoisomerase I-DNA cleavable complexes as a mechanism of cell killing by camptothecin. *Cancer Res* 49(18):5077–5082.
9. Ryan AJ, Squires S, Strutt HL, Johnson RT (1991) Camptothecin cytotoxicity in mammalian cells is associated with the induction of persistent double strand breaks in replicating DNA. *Nucleic Acids Res* 19(12):3295–3300.

10. Tsao YP, Russo A, Nyamuswa G, Silber R, Liu LF (1993) Interaction between replication forks and topoisomerase I-DNA cleavable complexes: studies in a cell-free SV40 DNA replication system. *Cancer Res* 53(24):5908–5914.
11. Kathe SD, Shen G-P, Wallace SS (2004) Single-stranded breaks in DNA but not oxidative DNA base damages block transcriptional elongation by RNA polymerase II in HeLa cell nuclear extracts. *J Biol Chem* 279(18):18511–18520.
12. Zhou W, Doetsch PW (1993) Effects of abasic sites and DNA single-strand breaks on prokaryotic RNA polymerases. *Proc Natl Acad Sci USA* 90(14):6601–6605.
13. Date H, et al. (2001) Early-onset ataxia with ocular motor apraxia and hypoalbuminemia is caused by mutations in a new HIT superfamily gene. *Nat Genet* 29(2):184–188.
14. Moreira MC, et al. (2001) The gene mutated in ataxia-ocular apraxia 1 encodes the new HIT/Zn-finger protein aprataxin. *Nat Genet* 29(2):189–193.
15. Shen J, et al. (2010) Mutations in PNKP cause microcephaly, seizures and defects in DNA repair. *Nat Genet* 42(3):245–249.
16. El-Khamisy SF, et al. (2005) Defective DNA single-strand break repair in spinocerebellar ataxia with axonal neuropathy-1. *Nature* 434(7029):108–113.
17. Hoch NC, et al. (2016) XRCC1 mutation is associated with PARP1 hyperactivation and cerebellar ataxia. *Nature* 541(7635):87–91.
18. Bras J, et al. (2015) Mutations in PNKP cause recessive ataxia with oculomotor apraxia type 4. *Am J Hum Genet* 96(3):474–479.
19. Takashima H, et al. (2002) Mutation of TDP1, encoding a topoisomerase I-dependent DNA damage repair enzyme, in spinocerebellar ataxia with axonal neuropathy. *Nat Genet* 32(2):267–272.
20. Lee Y, et al. (2009) The genesis of cerebellar interneurons and the prevention of neural DNA damage require XRCC1. *Nat Neurosci* 12(8):973–980.
21. Aredia F, Scovassi AI (2014) Poly(ADP-ribose): a signaling molecule in different paradigms of cell death. *Biochem Pharmacol* 92(1):157–163.
22. Andrabi SA, et al. (2014) Poly(ADP-ribose) polymerase-dependent energy depletion occurs through inhibition of glycolysis. *Proc Natl Acad Sci USA* 111(28):10209–10214.
23. Fouquerel E, et al. (2014) ARTD1/PARP1 negatively regulates glycolysis by inhibiting hexokinase 1 independent of NAD⁺ depletion. *Cell Rep* 8(6):1819–1831.

24. Yu S-W, et al. (2006) Apoptosis-inducing factor mediates poly(ADP-ribose) (PAR) polymer-induced cell death. *Proc Natl Acad Sci USA* 103(48):18314–18319.
25. Eliasson MJ, et al. (1997) Poly(ADP-ribose) polymerase gene disruption renders mice resistant to cerebral ischemia. *Nat Med* 3(10):1089–1095.
26. Zhang J, Dawson VL, Dawson TM, Snyder SH (1994) Nitric oxide activation of poly(ADP-ribose) synthetase in neurotoxicity. *Science* 263(5147):687–689.
27. Rulten SL, Caldecott KW (2013) DNA strand break repair and neurodegeneration. *DNA Repair (Amst)* 12(8):558–567.
28. Iyama T, Wilson DM (2013) DNA repair mechanisms in dividing and non-dividing cells. *DNA Repair (Amst)* 12(8):620–636.
29. Gunn BG, Baram TZ (2017) Stress and Seizures: Space, Time and Hippocampal Circuits. *Trends Neurosci* 40(11):667–679.
30. Buchhalter J, Cascino GD (2017) SUDEP: An important cause of premature mortality in epilepsy across the life spectrum. *Neurology* 89(2):114–115.
31. Smithson WH, Colwell B, Hanna J (2014) Sudden unexpected death in epilepsy: addressing the challenges. *Curr Neurol Neurosci Rep* 14(12):502–6.
32. Glasscock E (2014) Genomic biomarkers of SUDEP in brain and heart. *Epilepsy Behav* 38:172–179.
33. Lee Y, et al. (2012) Neurogenesis requires TopBP1 to prevent catastrophic replicative DNA damage in early progenitors. *Nat Neurosci* 15(6):819–826.
34. Kuzminov A (2001) Single-strand interruptions in replicating chromosomes cause double-strand breaks. *Proc Natl Acad Sci USA* 98(15):8241–8246.
35. Strumberg D, et al. (2000) Conversion of topoisomerase I cleavage complexes on the leading strand of ribosomal DNA into 5'-phosphorylated DNA double-strand breaks by replication runoff. *Mol Cell Biol* 20(11):3977–3987.
36. Arnaudeau C, Lundin C, Helleday T (2001) DNA double-strand breaks associated with replication forks are predominantly repaired by homologous recombination involving an exchange mechanism in mammalian cells. *J Mol Biol* 307(5):1235–1245.
37. Haber JE (1999) DNA recombination: the replication connection. *Trends Biochem Sci* 24(7):271–275.
38. Costes A, Lambert SAE (2012) Homologous recombination as a replication fork escort: fork-protection and recovery. *Biomolecules* 3(1):39–71.

39. Langelier M-F, Pascal JM (2013) PARP-1 mechanism for coupling DNA damage detection to poly(ADP-ribose) synthesis. *Curr Opin Struct Biol* 23(1):134–143.
40. Mandir AS, et al. (2000) NMDA but not non-NMDA excitotoxicity is mediated by Poly(ADP-ribose) polymerase. *J Neurosci* 20(21):8005–8011.
41. Meli E, et al. (2003) Poly(ADP-ribose) polymerase as a key player in excitotoxicity and post-ischemic brain damage. *Toxicol Lett* 139(2-3):153–162.
42. Kriaucionis S, Heintz N (2009) The nuclear DNA base 5-hydroxymethylcytosine is present in Purkinje neurons and the brain. *Science* 324(5929):929–930.
43. Li W, Liu M (2011) Distribution of 5-hydroxymethylcytosine in different human tissues. *J Nucleic Acids* 2011:870726.
44. Wang ZQ, et al. (1995) Mice lacking ADPRT and poly(ADP-ribosyl)ation develop normally but are susceptible to skin disease. *Genes Dev* 9(5):509–520.

Figure 1

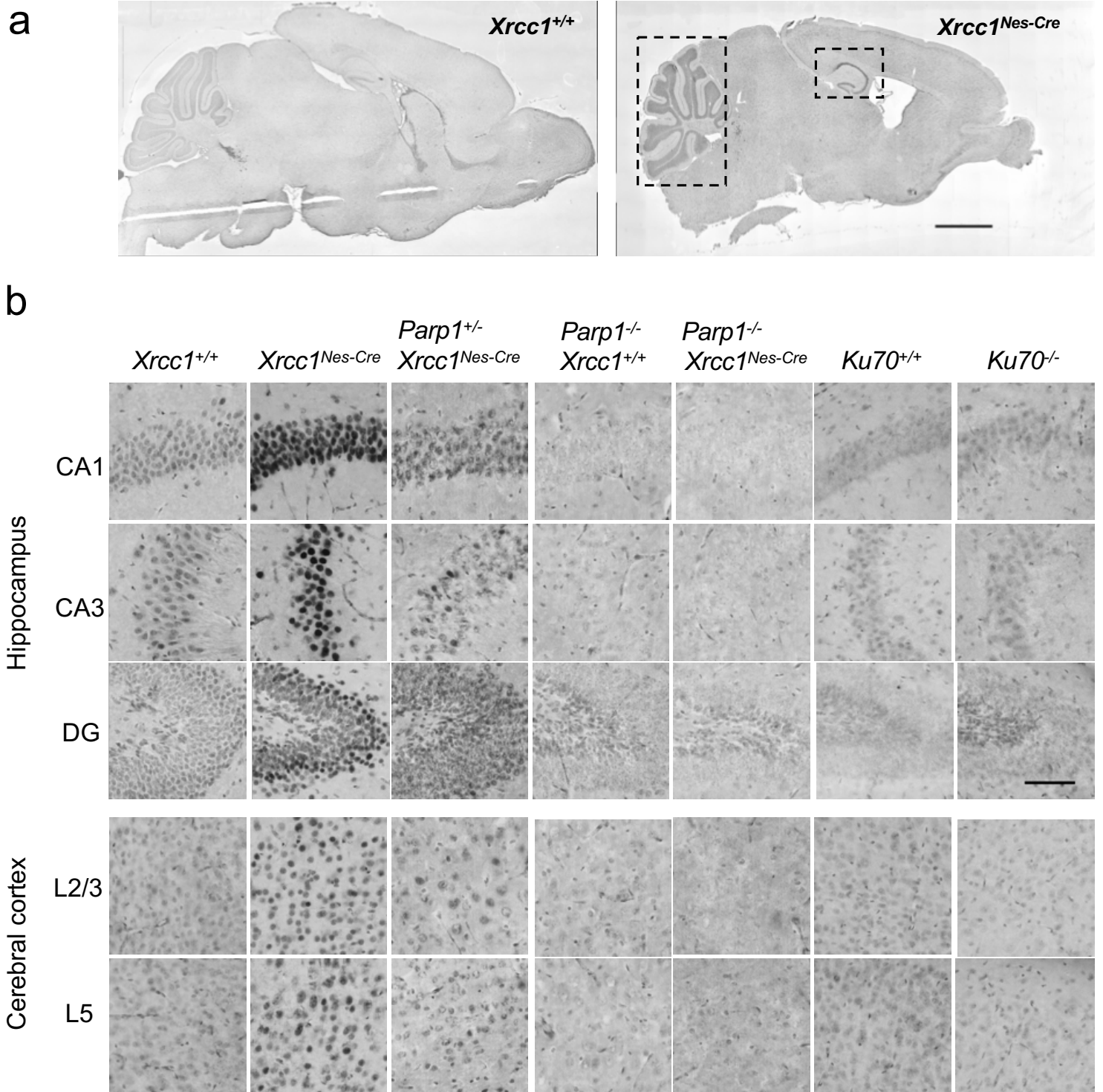


Figure 2

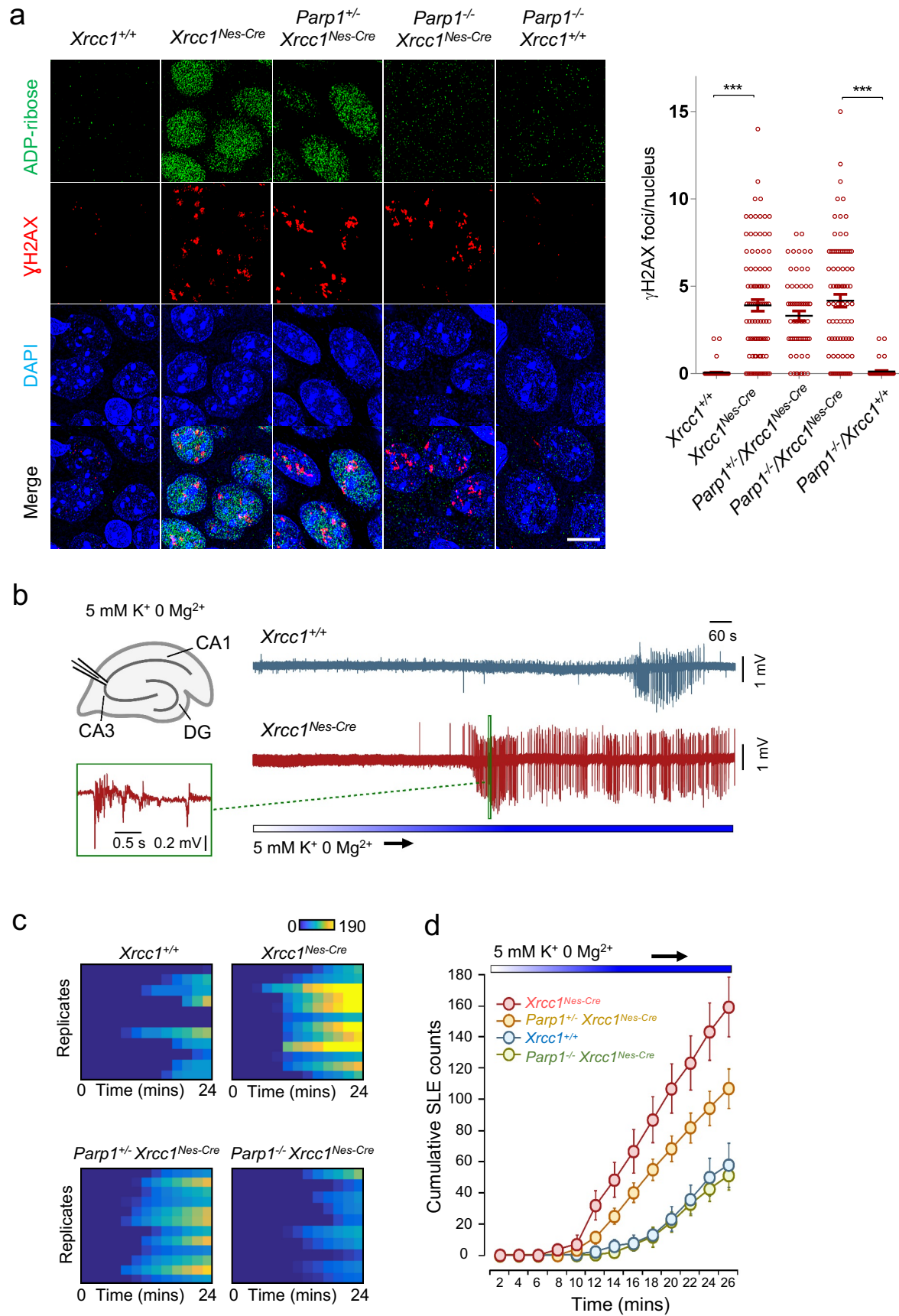
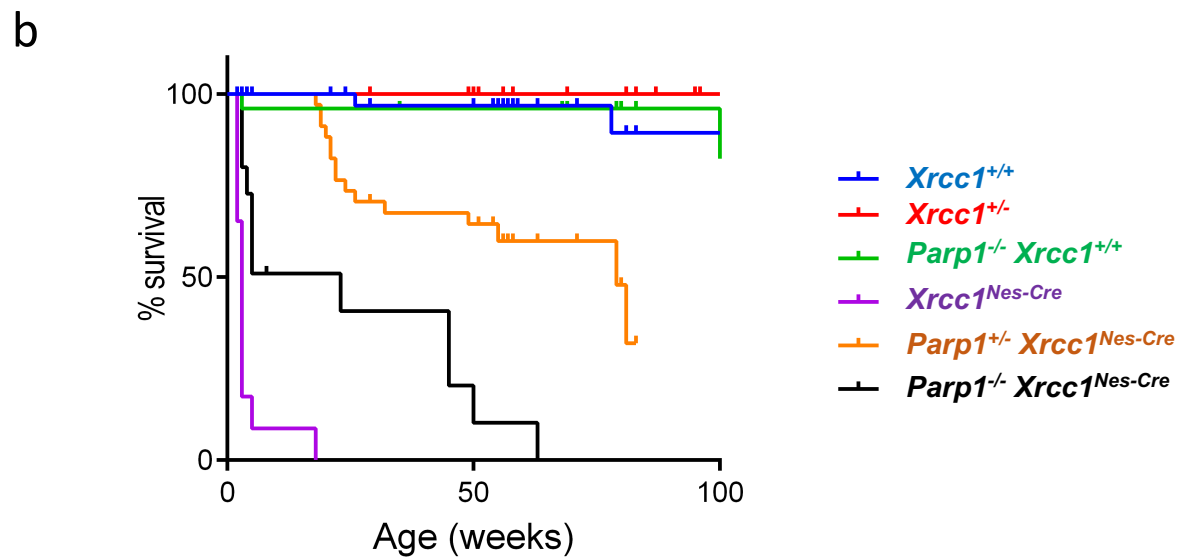
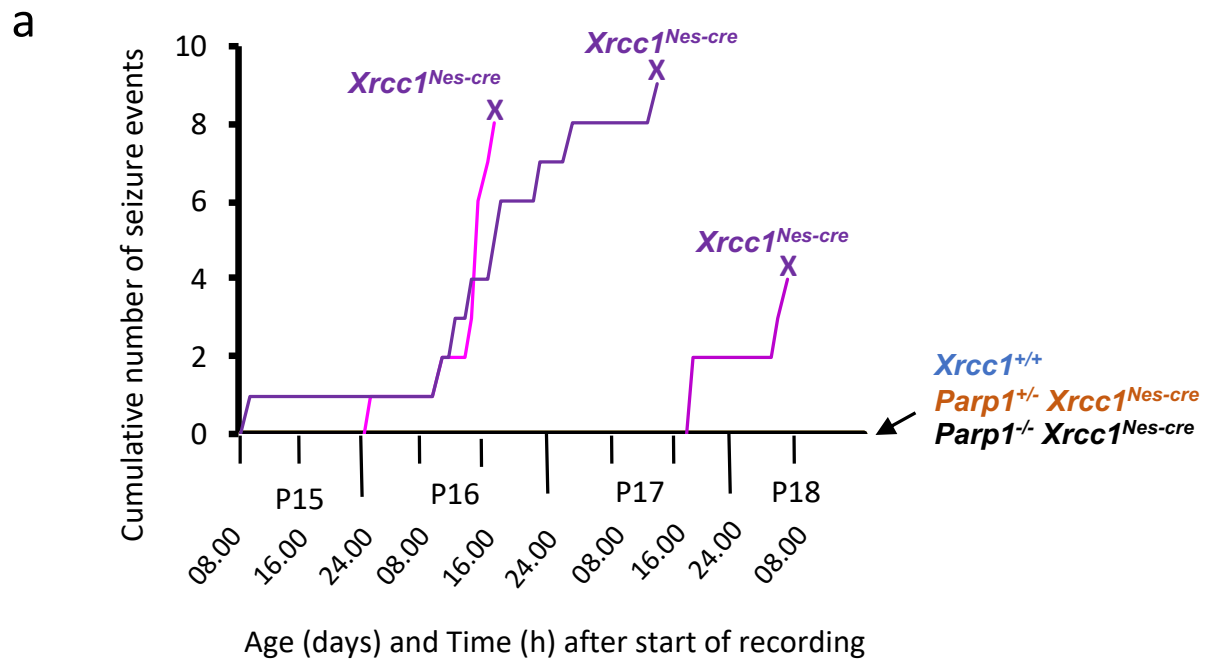


Figure 3



Genotype	n	Median survival	p vs WT	p vs <i>Xrcc1^{Nes-cre}</i>
<i>Xrcc1^{+/+}</i>	48	Und	-	<0.0001
<i>Xrcc1^{+/-}</i>	18	Und	ns	<0.0001
<i>Parp1^{-/-}</i>	25	Und	ns	<0.0001
<i>Xrcc1^{Nes-cre}</i>	23	3	<0.0001	-
<i>Parp1^{+/-} Xrcc1^{Nes-cre}</i>	35	79	<0.0001	<0.0001
<i>Parp1^{-/-} Xrcc1^{Nes-cre}</i>	15	23	<0.0001	<0.0001